

Available online at [www.sciencedirect.com](http://www.sciencedirect.com)

ScienceDirect

Procedia CIRP 62 (2017) 470 – 474

[www.elsevier.com/locate/procedia](http://www.elsevier.com/locate/procedia)

10th CIRP Conference on Intelligent Computation in Manufacturing Engineering - CIRP ICME '16

## Selection of optimal process parameters for wire arc additive manufacturing

Mariacira Liberini<sup>a</sup>, Antonello Astarita<sup>a,\*</sup>, Gianni Campatelli<sup>b</sup>, Antonio Scippa<sup>b</sup>, Filippo Montevecchi<sup>b</sup>, Giuseppe Venturini<sup>b</sup>, Massimo Durante<sup>a</sup>, Luca Boccarusso<sup>a</sup>, Fabrizio Memola Capece Minutolo<sup>a</sup>, A. Squillace<sup>a</sup>

<sup>a</sup>Department of Chemical, Materials and Industrial Production Engineering, University of Naples "Federico II", Piazzale Tecchio 80, 80125, Napoli, Italy

<sup>b</sup>Department of Industrial Engineering, University of Firenze, via di Santa Marta 3, Firenze 50139, Italy

\* Corresponding author. Tel.: +390817682555; fax: +390817682362. E-mail address: [antonello.atarita@unina.it](mailto:antonello.atarita@unina.it)

### Abstract

This paper is about the optimal selection of process parameters for Wire Arc Additive Manufacturing technology, an emerging solution for additive production of metal parts. In particular, the selection of the process parameters is based on the evolution of the microstructure and on the mechanical properties of the final samples obtained through the successive deposition weld beads of a ER70S-6 steel, according to the AWS legislation. The feed rate and the heat input during the deposition of the weld beads have been varied, in order to understand how the temperature reached by the samples can affect the final product mechanical characteristics. The final cooling has been carried in calm air at room temperature and between the deposition of a weld bead and the following one it has been imposed a pause of 60s. The tests on mechanical properties carried out have been: A full experimental campaign that includes: macrographic observations, micrographic observations and Vickers microhardness. The analysis of these tests has highlighted that by varying the process parameters, the samples do not have substantial differences between them. Instead, a microstructure that evolves from pearlitic-ferritic grains until bainitic lamellae along the vertical direction of the samples has been observed by micrographic analysis and confirmed by microhardness measurements.

© 2017 The Authors. Published by Elsevier B.V. This is an open access article under the CC BY-NC-ND license

(<http://creativecommons.org/licenses/by-nc-nd/4.0/>).

Peer-review under responsibility of the scientific committee of the 10th CIRP Conference on Intelligent Computation in Manufacturing Engineering

**Keywords:** Wire arc additive manufacturing; ER70S-6 Steel; Microstructure; Vickers hardness.

### 1. Introduction

Additive manufacturing techniques (AM) are widely used today in order to build up products by the deposition of materials layer-by-layer, instead of using traditional processing techniques based on the machining of the raw material. AM is a promising alternative for fabricating components made of expensive materials such as titanium or aluminum alloys, because of the high value of the buy-to-fly ratio. Many techniques have been developed for manufacturing metal structures in AM, such as selective laser sintering [1], direct metal deposition [2], electron beam melting [3], shape deposition manufacturing [4], and wire and arc additive manufacturing (WAAM) [5–7]. According to the different energy sources used for the deposition of the metal, wire-feed AM is classified into three groups: laser based, arc

welding based, and electron beam based [8]. Arc welding based AM has the advantages of a lower cost and higher deposition rate, achieved at the cost of lower feature resolution. This is not a problem for most of the products since a following machining operation is often due. Usually, the deposition rate of laser or electron beam deposition is about 2–10 g/min, while for the arc welding technology the deposition rate is about 50–130 g/min [9–11]. In WAAM, the building strategy consists in the deposition of a series of single weld beads, one on the other, alternating pauses of cooling with deposition steps [12]. The following work is based on the deposition of successive layers of low carbon steel. Heating and cooling phases of the process affects the microstructure and the mechanical characteristics of product [13], that have a strong influence on issues like material machinability [14] and fatigue strength. So, it is really

important to define the effect of process parameters on the final microstructure of the product obtained in order to choose the optimal setup. The process parameters varied within the tests has been chosen in order to vary both the heat input of the process and the heat flux in a specific product area.

**2. Experimental**

The experimental campaign for the study and the characterization of the specimens obtained by WAAM technique consists in:

- Macrographic Observations
- Micrographic Analysis by Scanning Electron Microscope
- Vickers microhardness
- Surface analysis by confocal microscopy

The test samples were made by depositing successive layers of materials on a low carbon steel substrate. The filler material used is a standard filler for welding structural steels: ER70S-6 designation according AWS legislation. The test samples were made by superimposing 15 layers. A pause of 60s was imposed between each layer deposition, in order to enable a partial cooling of the deposited material. In the execution of the specimens it was maintained a distance of 10 mm between the torch and the work surface. The deposition procedure is shown in figure 1. Figure 2 shows the ID numbers of specimens and their positioning on the substrate. For the construction of the samples it was used a MIG / MAG welding Millermatic 300 (manufacturer: Miller), whose welding torch was moved by a three axes CNC machine. The tests were performed by setting the values of voltage, feed rate and wire feed speed, in order to obtain different values of heat input. In table 1 are reported the values of the process parameters for individual specimens. All the samples are cooled in calm air at room temperature.

Each sample was cut off from the substrate and it was cut in the middle of the superimposed weld beads in order to observe the bulk of the sample. Before the observations and the analysis, each sample was first grinded by P320 emery paper and then polished by three different diamond suspensions: 9µm, 3 µm, 1 µm and finally ultrasonically cleaned in acetone for 10 min to avoid the presence of impurities. The samples were first observed with a ZEISS Axioplan 2 microscope in order to find the characteristic zones of the samples, then each zone of each sample was analyzed with the Scanning Electron Microscope (SEM) Hitachi TM3000. After the macro and the micro analysis, Vickers microhardness measures were performed along the length of each sample, in order to evaluate the hardness from the first layer deposited on the substrate to the last one, with the CV-400DAT micro Vickers Hardness tester, a load of 300g applied for 20s was used. At last, the ripple surface of each sample was detected with the Confocal Leica DCM3D microscope, to calculate the distance between the deepest valley and the highest peak. The ripple surface was calculated with the external surface of each sample and it was elaborated with the LeicaMap software through operations of filling, leveling and filtering.

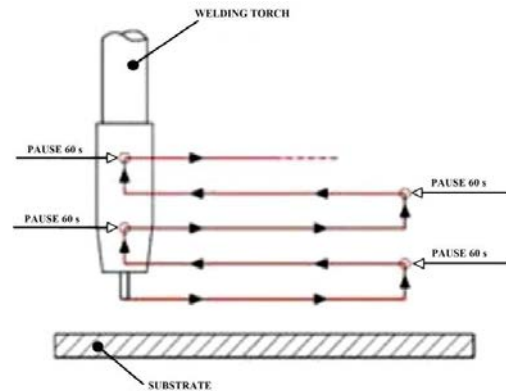


Fig. 1 - Strategy of deposition of the layers. The 60s pause is highlighted.

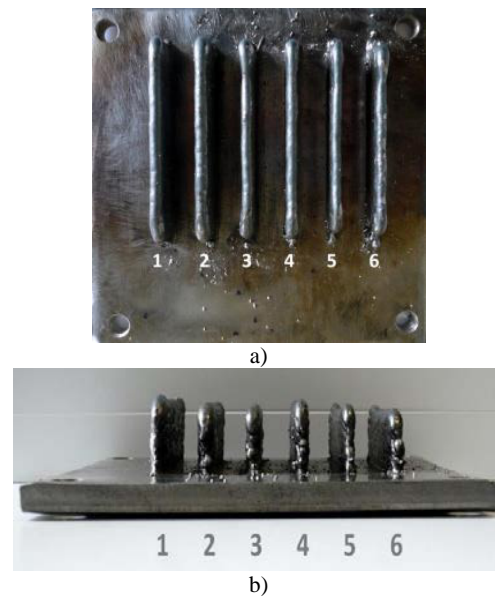


Fig. 2 - Nesting of the samples on the substrate

Tab. 1 - Process parameters of the welding process relative to each sample

Sample	Current [A]	Voltage [V]	Wire Speed [m/min]	Speed Rate [mm/min]	Heat Input [J/m]
1	50	11,7	1,68	300	11707
2	50	13,1	1,68	300	13084
3	50	13,1	1,68	375	10467
4	50	11,7	1,68	375	9365
5	50	11,7	1,68	450	7805
6	50	13,1	1,68	450	8723

**3. Results**

In the hereinafter the microstructures of the different samples will be discussed. In all the samples three different zones can be observed: the lower zone, the middle zone, the upper zone. The lower zones is characterized by being in contact with the cold substrate before the deposition, the middle zone is characterized by the lower thermal shock, since the substrate of that zone is a warm weld bead

deposited, finally the upper zone shows the higher value of thermal shock because of the contact with the calm air at room temperature. In particular, in Fig. 3, the macrographs of the three different zones are reported. It can be noticed the substantial difference between the microstructure of the upper zone with respect to the other two zones. The lower and the middle areas are in fact characterized by a roughly equiaxed microstructure, while the upper zones shows a lamellar microstructure. In Fig.4 it can be noted a macrography in which a transition from the lower zone to the middle zone is reported. In that macrography it is possible to note the presence of a mix microstructure in the lower zone and also of the finer particle size with respect to the middle zone. Thanks to the micrographic analysis, the zones found in the previous macrographs can better identify and classify. In Fig. 5.a a micrograph on the lower zone is shown. It is possible to observe equiaxed grains in which thin lamellae are dispersed [13, 15]. Given the initial thermal shock due to the contact with the cold substrate it is possible to say that this microstructure is characterized by the ferrite grains and by the pearlite lamellae. The material is a mild carbon steel and this justified the fact that the ferrite coexists in equiaxed form with the thin strips of pearlite [13, 15]. In Fig. 5.b is shown a micrograph of the middle zone. The middle zone is characterized by equiaxed grains of pure ferrite. It is possible to observe from the micrographs, that the crystal grain size of the middle zone is coarser than the one of the lower zone and this is due to the higher value of the thermal shock of the lower zone with respect to the middle zone. The middle zone undergoes a slow cooling rate with respect to the upper areas, but the thermal gradient is lower than in the lower zone. The lower zone suffers a slow cooling with respect to the upper zone and this explains the ferrite, while the partial thermal shock due to the cold substrate justifies the presence of pearlite. Finally, in Fig. 5.c, a micrograph of the upper zone is shown. As already mentioned, this is the area that manifests a higher value of thermal shock and thus the microstructure is completely different and it is of the lamellar type. In particular, it is possible to distinguish that the microstructure consists of bainite laths aggregate composed of both ferrite and cementite. As the cooling starts from a temperature of about  $70^\circ$  greater than the critical one for the used steel, it is justified the growth of ferrite laths devoid of carbon. In fact, since the carbon in the ferrite is contained in smaller quantities, it migrates on the upper areas and the laths are filled with carbon. The average dimension of the grain size is calculated with the ASTM standard and the values of the size of the grains are reported in Tab. 2. In Fig. 6 a graphic with the values of the Vickers microhardness values is reported. The prints are taken as described in literature. The results show the values of the microhardness from the lower zone to the upper zone and as it can be observed the higher value of the microhardness belongs to the bainite microstructure. There are no significant differences between the samples processed with different process parameters, but it is remarkable that there is no porosity, and this fact is a relevant advantage with respect to the others Additive Manufacturing techniques.

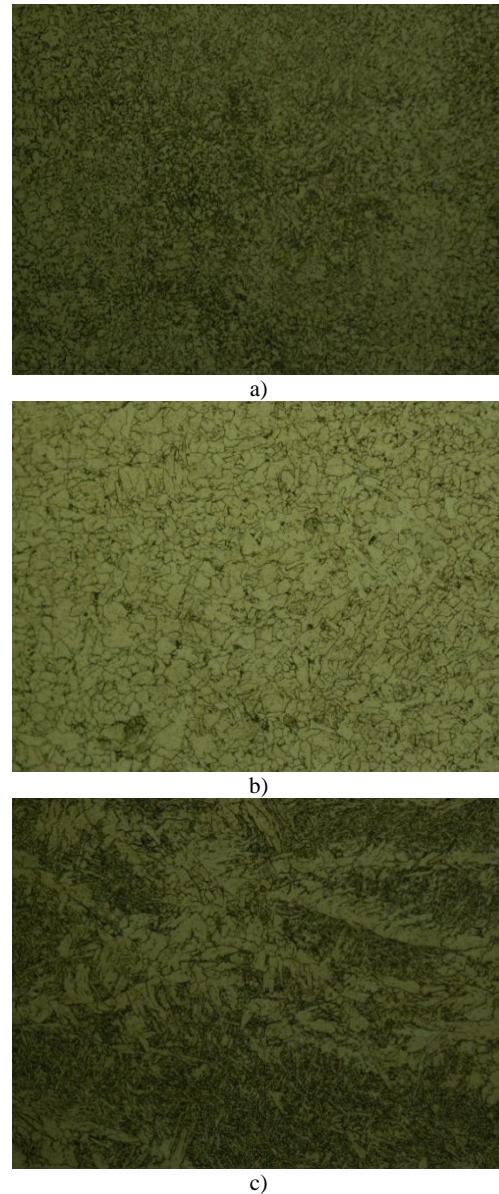


Fig. 3 - 3.a Macrography of the pearlitic/ferritic lower zone, 3.b Macrography of the ferritic middle zone, 3.c Macrography of the bainitic upper zone

Moreover, it is possible to get different microstructures along the height of the specimen, due to the reheating effect induced by the layer stacking. This effect opens the possibility to adjust the bainite/ferrite structure according to the needs required in terms of formability and mechanical performances alternating cycles of cooling with water or oil after the deposition of one or more layers. Finally, there are no substantial differences in the samples obtained by varying the process parameters, since the microstructural evolution of steel depends on parameters that are directly related to the process setup but are: the chemical composition, the cooling curve in time, the maximum temperature reached in the process. In this case the involved technology does not change the chemical structure



of the product, the maximum temperature reached in the different samples is roughly the same since it is only lightly affected by the heat input of the source, but above all, the cooling is the same for each specimen (in calm air at room temperature) since it is related mainly to the geometry of the product and the dimension of the surface. This is really important, since the cooling curve is the factor that most influences the final microstructure. Given this background, it is justifiable that there are no large variations between the samples obtained from different process parameters.

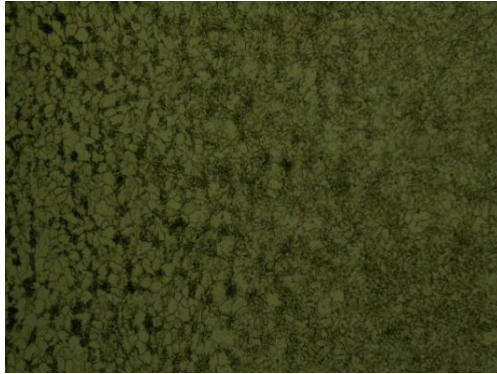
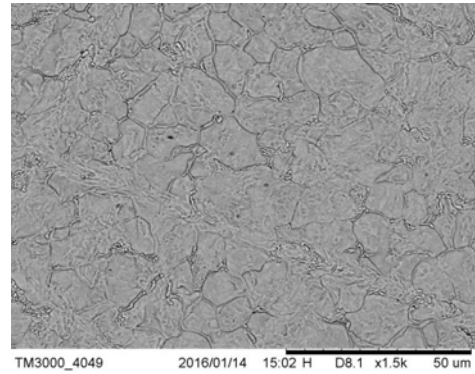


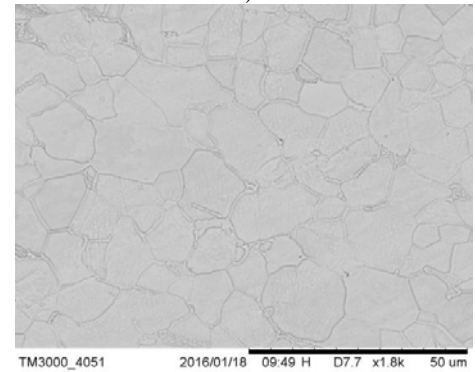
Fig.4 - Transition zone between the lower and the middle zone in which is possible to observe the difference of the microstructure between the lower and the middle zone and the difference of the grain size between the two zones

Tab.2 - Average values of the grain size in the different zones of the samples

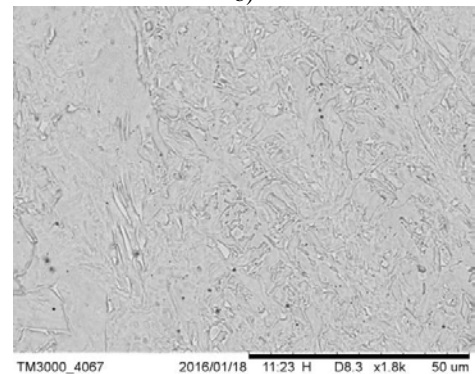
Zone of the Sample	Mean Grain Size [um]
Lower zone (grain size)	17.8
Middle zone (grain size)	22.1
Upper zone (measure of the length of the laths)	32.5



a)



b)



c)

Fig. 5- 5.a Micrography of the pearlitic/ferritic lower zone, 5.b Micrography of the ferritic middle zone, 5.c Micrography of the bainitic upper zone

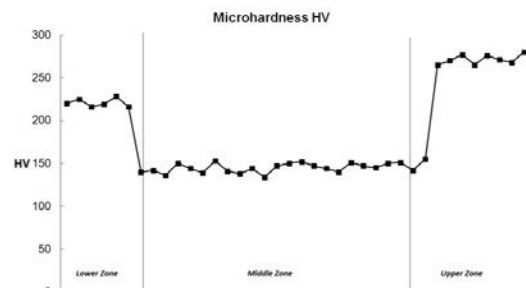


Fig. 6 - Vickers Microhardness values in the three different zones of the samples

#### 4. Conclusions

The study of samples produced by Wire Arc Additive Manufacturing technology has led to the following conclusions:

- There are no substantial differences between the samples processed with different process parameters due to the preeminence of cooling curve on the product microstructure, that is not affected by process parameters.
- In all the samples have been noted three different zones: the lower zone characterized by a ferritic structure with thin strips of pearlite, the middle zones characterized by equiaxed grains of ferrite and the upper zone characterized by a lamellar structure typically bainitic.
- The difference in the three found microstructures is due to the different thermal history experienced by the different welding beads deposited, in which the upper zone is affected by the stronger thermal shock.
- The particle size is finer in the lower zone as the lower zone experiences a higher value of thermal shock than the middle zone that has a coarse value grain sizes.
- The Vickers microhardness confirm with their values the different microstructures found in samples.

In addition based on the results of the present research activity, it could be suggested a strategy to obtain a structure ferrite/bainite according to the needs required by the final product, that could be obtained alternating cooling cycles with water or oil between and the deposition of the weld beads.

#### References

- [1] Agarwala M, Bourell D, Beaman J, Marcus H, Barlow J. Direct selective laser sintering of metals. *Rapid Prototyp J* 1995;1:26–36.
- [2] Lewis GK, Schlienger E. Practical considerations and capabilities for laser assisted direct metal deposition. *Mater Des* 2000;21:417–23.
- [3] Taminger KM, Hafley RA. Electron beam freeform fabrication: a rapid metal deposition process. In: *Proceedings of the 3rd annual automotive composites conference*; 2003. p. 9–10.
- [4] Merz R, Prinz FB, Ramaswami K, Terk M, Weiss L. *Shape deposition manufacturing: engineering design research center*. Stanford, California, USA: Carnegie Mellon University; 1994.
- [5] Almeida PS, Williams S. Innovative process model of Ti–6Al–4V additive layer manufacturing using cold metal transfer (CMT). In: *Proceedings of the twenty-first annual international solid freeform fabrication symposium*. Austin, TX, USA: University of Texas; 2010.
- [6] Ding J, Colegrove P, Mehnen J, Ganguly S, Sequeira PM, Wang F, et al. Thermomechanical analysis of wire and arc additive layer manufacturing process on large multi-layer parts. *Comput Mater Sci* 2011;50:3315–22.
- [7] Wang F, Williams S, Rush M. Morphology investigation on direct current pulsed gas tungsten arc welded additive layer manufactured Ti6Al4V alloy. *Int J Adv Manuf Technol* 2011;57:597–603.
- [8] Mok SH, Bi G, Folkes J, Pashby I. Deposition of Ti–6Al–4V using a high power diode laser and wire, Part I: investigation on the process characteristics. *Surf Coat Technol* 2008;202:3933–9.
- [9] Brandl E, Michailov V, Viehweger B, Leyens C. Deposition of Ti–6Al–4V using laser and wire, part I: microstructural properties of single beads. *Surf Coat Technol* 2011;206:1120–9.
- [10] Zhang Y, Wei Z, Shi L, Xi M. Characterization of laser powder deposited Ti–TiC composites and functional gradient materials. *J Mater Process Technol* 2008;206:438–44.
- [11] Karunakaran KP, Suryakumar S, Pushpa V, Akula S. Low cost integration of additive and subtractive processes for hybrid layered manufacturing. *Robot Comput-Integr Manuf* 2010;26:490–9. Fig. 13. Experiments of multi-bead and multi-layer deposition. D. Ding et al. / *Robot Cim-Int Manuf.* (2015) 101–110 109.
- [12] Mazumder J, Dutta D, Kikuchi N, Ghosh A. Closed loop direct metal deposition: art to part. *Opt Lasers Eng* 2000;34:397–414
- [13] Donghong Ding, Zengxi Pan, Dominic Cuiuri, Huijun Li, A multi-bead overlapping model for robotic wire and arc additive manufacturing (WAAM) *Robot Cim-Int Manuf.* 31 (2015) 101-110
- [14] Filippo Montevercchi, Niccolò Grossi, Hisataka Takagi, Antonio Scippa, Hiroyuki Sasahara, Gianni Campatelli, Cutting Forces Analysis in Additive Manufactured AISI H13 Alloy, *Procedia CIRP*, Volume 46, 2016, Pages 476-479, ISSN 2212-8271, <http://dx.doi.org/10.1016/j.procir.2016.04.034>.
- [15] American Society for Metals, *Metals Handbook Ninth Edition* 1988